

QCD CORRECTIONS AND LLA QED CORRECTIONS

HECTOR WS

J BLÜMLEIN

1. STRUCTURE FUNCTIONS
2. QCD CORRECTIONS
3. LOW Q^2 σ
4. LLA QED
 - 4.1. $O(\alpha_L)$
 - 4.2. HIGHER ORDERS

Structure Functions

$$F_2(x, Q^2) = x \sum_q |Q_q|^2 [q(x, Q^2) + \bar{q}(x, Q^2)],$$

$$G_2(x, Q^2) = x \sum_q |Q_q| v_q [q(x, Q^2) + \bar{q}(x, Q^2)],$$

$$H_2(x, Q^2) = x \sum_q \frac{1}{4} (v_q^2 + a_q^2) [q(x, Q^2) + \bar{q}(x, Q^2)],$$

$$xG_3(x, Q^2) = x \sum_q |Q_q| a_q [q(x, Q^2) - \bar{q}(x, Q^2)],$$

$$xH_3(x, Q^2) = x \sum_q \frac{1}{2} v_q a_q [q(x, Q^2) - \bar{q}(x, Q^2)]$$

$$\begin{aligned} v_f &= 1 - 4|Q_f| \sin^2 \theta_W^{\text{eff}}, \\ a_f &= 1. \end{aligned}$$

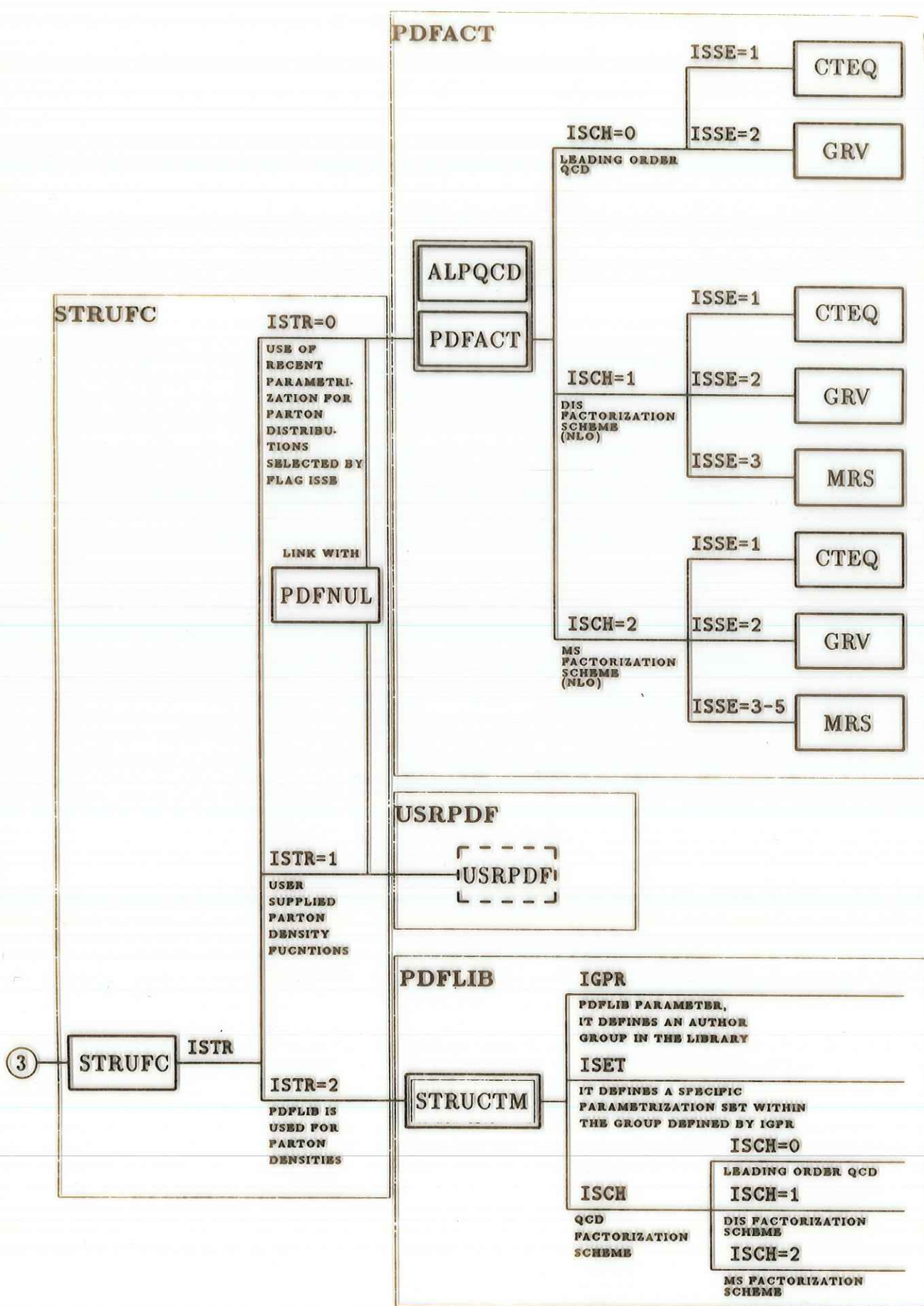
$$W_2^+(x, Q^2) = 2x \sum_i [d_i(x, Q^2) + \bar{u}_i(x, Q^2)],$$

$$W_2^-(x, Q^2) = 2x \sum_i [u_i(x, Q^2) + \bar{d}_i(x, Q^2)],$$

$$xW_3^+(x, Q^2) = 2x \sum_i [d_i(x, Q^2) - \bar{u}_i(x, Q^2)],$$

$$xW_3^-(x, Q^2) = 2x \sum_i [u_i(x, Q^2) - \bar{d}_i(x, Q^2)]$$

$$2x\mathcal{S}_1 = \mathcal{S}_2 - \mathcal{S}_L$$



QCD corrections

The strong coupling constant

$\overline{\text{MS}}$ renormaliz.

$$\begin{aligned}\alpha_s^{\text{LO}}(Q^2) &= \frac{4\pi}{\beta_0 \ln(Q^2/\Lambda^2)}, \\ \alpha_s^{\text{NLO}}(Q^2) &= \alpha_s^{\text{LO}}(Q^2) \left[1 - \frac{\beta_1}{\beta_0^2} \frac{\ln \ln(Q^2/\Lambda^2)}{[\ln(Q^2/\Lambda^2)]^2} \right],\end{aligned}$$

$$\begin{aligned}\beta_0 &= 11 - \frac{2}{3} N_f, \\ \beta_1 &= 102 - \frac{38}{3} N_f.\end{aligned}$$

Parton distributions in the $\overline{\text{MS}}$ factorization scheme

$$\begin{aligned}q_{ij}^+(x, Q^2) &= q_{ij}^+(x, Q^2)_{\overline{\text{MS}}} + \frac{\alpha_s(Q^2)}{2\pi} \left\{ \int_x^1 \frac{dy}{y} \left[\frac{x}{y} C_q \left(\frac{x}{y} \right) [q_{ij}^+(y, Q^2)_{\overline{\text{MS}}} - q_{ij}^+(x, Q^2)_{\overline{\text{MS}}}] \right. \right. \\ &\quad \left. \left. + 2 \frac{x}{y} C_g \left(\frac{x}{y} \right) \mathcal{G}(y, Q^2)_{\overline{\text{MS}}} \right] - q_{ij}^+(x, Q^2)_{\overline{\text{MS}}} \int_0^x dy C_q(y, Q^2) \right\},\end{aligned} \quad (2.73)$$

where

$$\mathcal{G} \equiv x G, \quad (2.74)$$

$$C_q(z) = C_F \left[\frac{1+z^2}{1-z} \left(\ln \frac{1-z}{z} - \frac{3}{4} \right) + \frac{1}{4} (9+5z) \right], \quad (2.75)$$

$$C_g(z) = \frac{1}{2} \left\{ [z^2 + (1-z)^2] \ln \frac{1-z}{z} + 8z(1-z) - 1 \right\}, \quad (2.76)$$

with $C_F = (N_c^2 - 1)/(2N_c) \equiv 4/3$ and

Correspondingly q_{ij}^- is

$$q_{ij}^-(x, Q^2) = x [q_i(x, Q^2) - \bar{q}_j(x, Q^2)]. \quad (2.77)$$

For this combination one has

$$\begin{aligned}q_{ij}^-(x, Q^2) &= q_{ij}^-(x)_{\overline{\text{MS}}} + \frac{\alpha_s(Q^2)}{2\pi} \left\{ \int_x^1 \frac{dy}{y} \frac{x}{y} \left[C_3 \left(\frac{x}{y} \right) q_{ij}^-(y, Q^2)_{\overline{\text{MS}}} - C_q \left(\frac{x}{y} \right) q_{ij}^-(x, Q^2)_{\overline{\text{MS}}} \right] \right. \\ &\quad \left. - q_{ij}^-(x, Q^2)_{\overline{\text{MS}}} \int_0^x dy C_q(y) \right\},\end{aligned} \quad (2.78)$$

$$C_3(z) = C_q(z) - (1+z)C_F.$$

Finally, for the longitudinal structure function, the correction reads

$$q_{ij}^L(x, Q^2) = \frac{\alpha_s(Q^2)}{2\pi} \int_x^1 \frac{dy}{y} \left(\frac{x}{y}\right)^2 \left\{ 2C_F q_{ij}^+(y, Q^2)_{\overline{\text{MS}}} + 4 \left(1 - \frac{x}{y}\right) \mathcal{G}(y, Q^2)_{\overline{\text{MS}}} \right\}.$$

Parton distributions in the DIS factorization scheme

The $+$ distributions eq. (2.68) are associated with the coefficient function

$$\delta(1-z) \quad (2.81)$$

in the DIS scheme. Thus the generalized structure functions $\mathcal{F}_2, \mathcal{G}_2, \mathcal{H}_2, \mathcal{W}_2$, are just linear combinations of the quark quark distributions in the DIS scheme. The generalized structure functions $\mathcal{G}_3, \mathcal{H}_3, \mathcal{W}_3$, on the other hand, constitute of lineare combinations of

$$q_{ij}^-(x, Q^2) = q_{ij}^-(x, Q^2)_{\text{DIS}} + \frac{\alpha_s(Q^2)}{2\pi} \int_x^1 \frac{dy}{y} \frac{x}{y} C_3^{\text{DIS}} \left(\frac{x}{y}\right) q_{ij}^-(y, Q^2)_{\text{DIS}}. \quad (2.82)$$

with

$$C_3^{\text{DIS}}(z) = -C_F(1+z). \quad (2.83)$$

ISSE	ISCH	σ_B [nb]	$\delta_{\text{ini}}^{(1)}$ [%]
1	0	0.2246E+06	13.01
2	0	0.2441E+06	12.94
1	1	0.2225E+06	12.65
3	1	0.2679E+06	11.76
1	2	0.2345E+06	12.82
2	2	0.2702E+06	12.13
3	2	0.2695E+06	11.84
4	2	0.2410E+06	13.56
5	2	0.2415E+06	13.55

Table 3: Born cross sections for unpolarized e^+p scattering with NTLO QCD corrections for different sets of parton parameterizations. Parameters: $x = 10^{-3}$, $y = 0.1$, $E_e = 26.7$ GeV, $E_p = 820.0$ GeV, and IVPL=1 (i.e. running α). The low Q^2 damping corresponds to IVAR=0.

2.4 Low Q^2 modifications of structure functions and parton distributions

$$\begin{aligned}\mathcal{F}_{1,2}(x, Q^2) &\rightarrow F_{\text{var}} \mathcal{F}_{1,2}(x, Q^2), \\ F_{\text{var}} &= [1 - \exp(-aQ^2)], \quad a = 3.37 \text{ GeV}^{-2}.\end{aligned}$$

Other approaches have a similar form:

$$F_{\text{var}}(Q^2) = [1 - W_2^{\text{el}}(Q^2)].$$

Parametrizations of the elastic form factor W_2^{el} ,

$$\begin{aligned}W_2^{\text{el}}(Q^2) &= \frac{G_e^2 + \tau G_m^2}{1 + \tau}, \\ \tau &= \frac{Q^2}{4M^2},\end{aligned}$$

IVAR	σ_B [nb]	$\delta_{\text{ini}}^{(1)}$ [%]
-1	0.4026E+08	9.452
0	0.3816E+08	9.222
1	0.3616E+08	9.197
2	0.7445E+07	32.53

Table 4: Born cross sections for e^+p scattering with different parton distribution parameterizations at low Q^2 . Parameters: $x = 10^{-4}$, $y = 0.1$, $E_e = 26.7$ GeV, $E_p = 820.0$ GeV, ISSE=1, ISCH=0, IVPL=1.

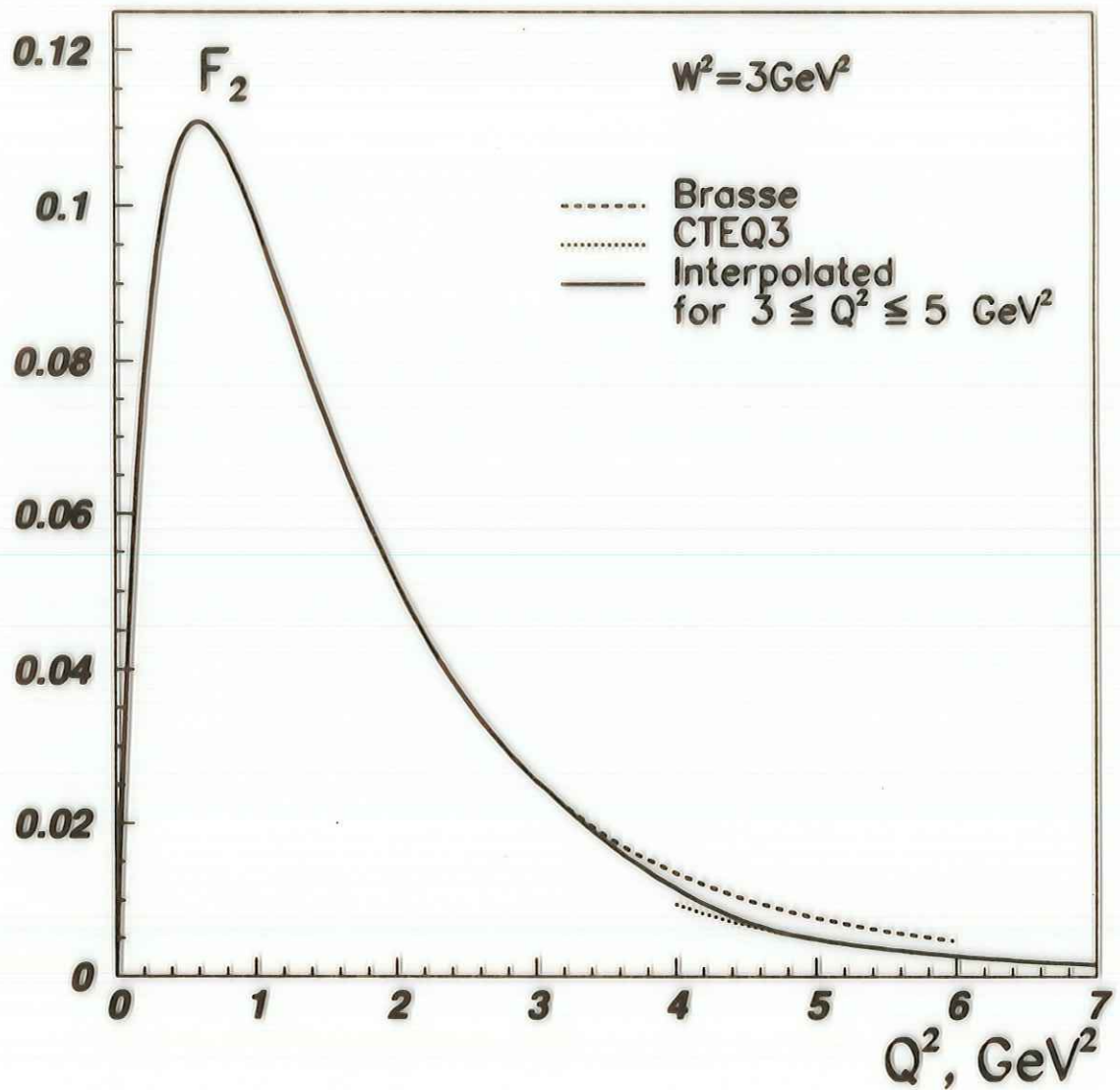


Figure 1: Low Q^2 interpolation for the structure function $F_2(x, Q^2)$ between $F_2 = F_2^{LO}(\text{CTEQ3})$ for $Q^2 \geq 5 \text{ GeV}^2$ (`ISCH = 0, ISSE = 1`), and the low Q^2 extension selected by the flag `IVAR=2` for $Q^2 \leq 3 \text{ GeV}^2$.

QED: Leading Log terms

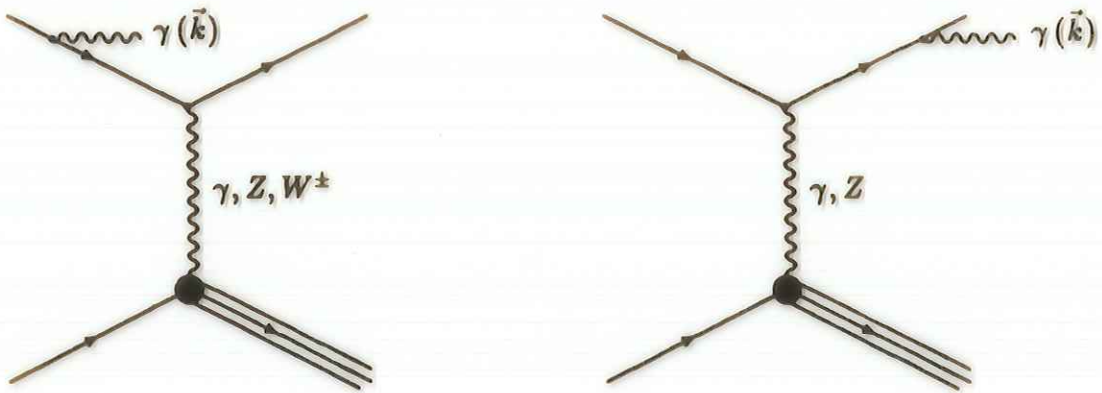


Figure 4: The leptonic QED bremsstrahlung diagrams

$$\frac{d^2\sigma^{LLA}}{dxdy} = \frac{d^2\sigma^0}{dxdy} + \frac{d^2\sigma^{ini,1loop}}{dxdy} + \frac{d^2\sigma^{ini,2loop}}{dxdy} + \frac{d^2\sigma^{ini,>2,soft}}{dxdy} + \frac{d^2\sigma^{ini,e^- \rightarrow e^+}}{dxdy} + \frac{d^2\sigma^{fin,1loop}}{dxdy} + \frac{d^2\sigma^C}{dxdy}.$$

$O(\alpha L)$

$$\frac{d^2\sigma^{ini(fin),1loop}}{dxdy} = \frac{\alpha}{2\pi} L_e \int_0^1 dz P_{ee}^{(1)} \left\{ \theta(z - z_0) \mathcal{J}(x, y, Q^2) \left. \frac{d^2\sigma^0}{dxdy} \right|_{z=\hat{z}, y=\hat{y}, S=\hat{S}} - \frac{d^2\sigma^0}{dxdy} \right\}, \quad (2.96)$$

$$P_{ee}^{(1)} = \frac{1+z^2}{1-z}. \quad (2.97)$$

Here, we introduced the notion

$$L_e = \ln \frac{Q^2}{m_e^2} - 1. \quad (2.98)$$

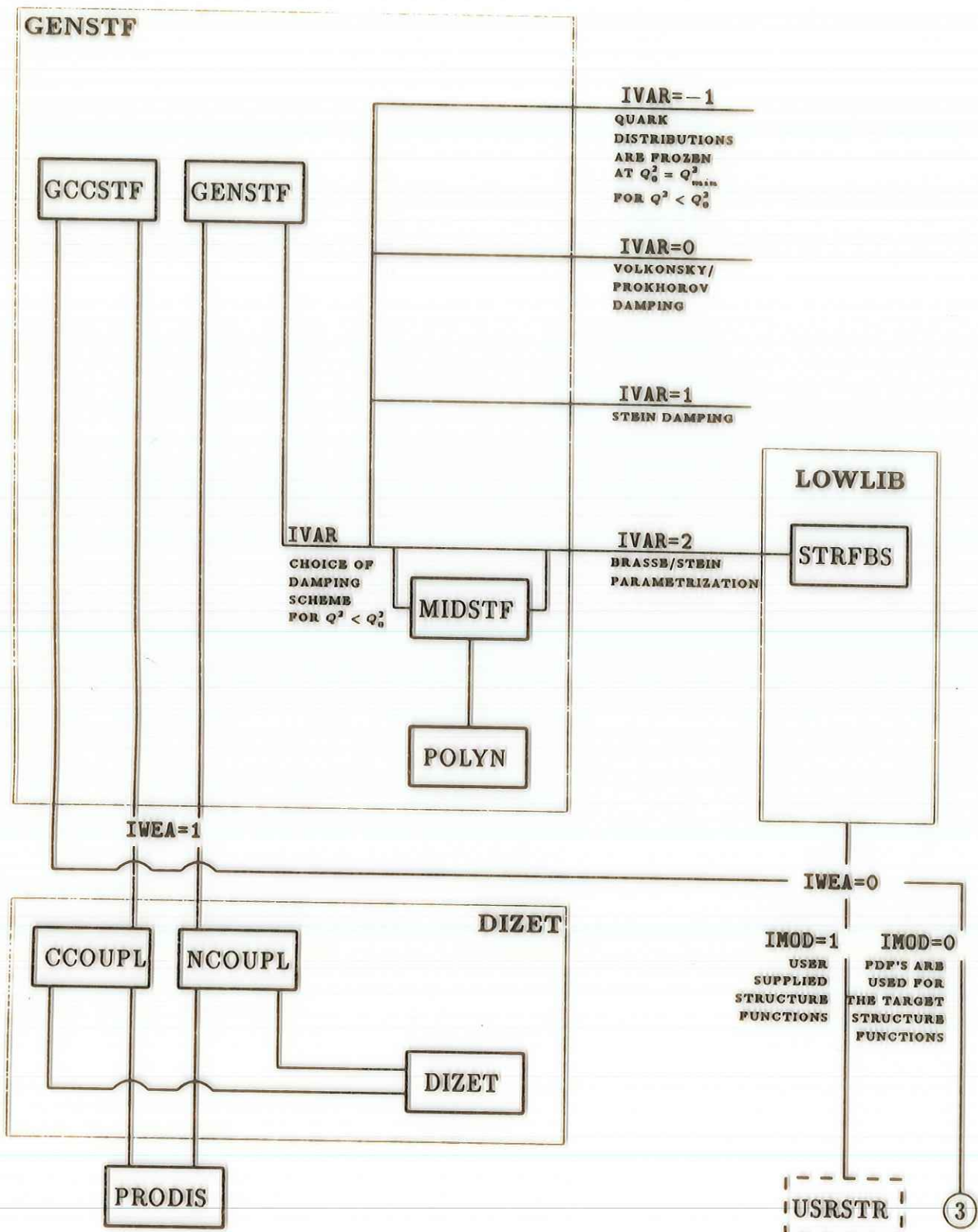


Figure 7: The logical structure of GENSTF

A Definition of scaling variables in presence of hard photon emission

In this appendix, we collect the definitions of all the sets of kinematical variables, which may be used in HECTOR. Some motivations for the specific choices may be found in [31]-[34].

Leptonic variables:

The scaling variables are defined from leptonic variables:

$$y_l = \frac{p_1(k_1 - k_2)}{p_1 k_1}, \quad (\text{A.1})$$

$$Q_l^2 = (k_1 - k_2)^2 = -2k_1 k_2, \quad (\text{A.2})$$

$$x_l = \frac{Q_l^2}{S y_l}. \quad (\text{A.3})$$

Hadronic variables:

The scaling variables are defined from hadronic variables:

$$y_h = \frac{p_1(p_2 - p_1)}{p_1 k_1}, \quad (\text{A.4})$$

$$Q_h^2 = (p_2 - p_1)^2, \quad (\text{A.5})$$

$$x_h = \frac{Q_h^2}{S y_h}. \quad (\text{A.6})$$

Jaquet-Blondel variables, [32]:

Again, the scaling variables are defined from hadronic variables. Using the transverse hadronic momentum in the laboratory system, \vec{p}_2^\perp , instead of p_2 and the energy flow in z direction in the definition of the scaling variables⁶:

$$y_{JB} = \frac{\Sigma}{2E_e} \quad (\text{A.7})$$

$$Q_{JB}^2 = \frac{(\vec{p}_{2\perp})^2}{1 - y_{JB}}, \quad (\text{A.8})$$

$$x_{JB} = \frac{Q_{JB}^2}{S y_{JB}}. \quad (\text{A.9})$$

with

$$\Sigma = \sum_h (E_h - p_{h,z}), \quad (\text{A.10})$$

Mixed variables, [33]:

The scaling variables are defined from both leptonic and Jaquet-Blondel variables:

$$Q_m^2 = Q_l^2, \quad (\text{A.11})$$

$$y_m = y_h, \quad (\text{A.12})$$

$$x_m = \frac{Q_l^2}{S y_h}. \quad (\text{A.13})$$

For mixed variables, the allowed values of x are not necessarily restricted to be smaller than one; see for details appendix B.3.1 of [10].

Σ method, [34]

The scaling variables are defined from both leptonic and hadronic variables as being measured in the laboratory system:

$$y_\Sigma = \frac{\Sigma}{\Sigma + E'_l(1 - \cos \theta_l)}, \quad (\text{A.14})$$

$$Q_\Sigma^2 = \frac{(\vec{k}_{2\perp})^2}{1 - y_\Sigma}, \quad (\text{A.15})$$

$$x_\Sigma = \frac{Q_\Sigma^2}{S y_\Sigma}, \quad (\text{A.16})$$

The value $z_0^{\Sigma,f}$ in the case of final state radiation is the solution of the equation

$$x[1 - y(1 - z_0)]^2 = z_0^3, \quad (\text{A.17})$$

$$z_0^{\Sigma,f} = E_1^{1/3} + E_2 E_1^{1/3} + \frac{1}{3} x y^2 \quad (\text{A.18})$$

with

$$E_1 = x(E_1^a + E_1^b) \quad (\text{A.19})$$

$$E_1^a = \frac{1}{2} - y \left(1 - \frac{1}{2}y - \frac{1}{27}x^2y^5 \right) + \frac{1}{3}xy^3(1-y), \quad (\text{A.20})$$

$$E_1^b = \frac{1}{6}\sqrt{9(1 - 4y + y^4) + 2y^2 \left[27 - 18y - \frac{2}{3}xy^4 + 2xy \left(\frac{1}{3} - y + y^2 \right) \right]}, \quad (\text{A.21})$$

$$E_2 = \frac{2}{3}xy \left(1 - y + \frac{1}{6}xy^3 \right). \quad (\text{A.22})$$

$e\Sigma$ method, [34]:

The $e\Sigma$ method mixes variables from the set of leptonic variables and of the Σ method:

$$Q_{e\Sigma}^2 = Q_l^2, \quad (\text{A.23})$$

$$x_{e\Sigma} = x_\Sigma, \quad (\text{A.24})$$

$$y_{e\Sigma} = \frac{Q_{e\Sigma}^2}{Sx_{e\Sigma}} = \frac{Q_l^2}{Sx_\Sigma}. \quad (\text{A.25})$$

The integration boundary $z_0^{\Sigma,f}$ is the same as in the Σ method.

Double angle method, [35]:

The scaling variables are defined from both leptonic and hadronic scattering angles as being measured in the laboratory system.

The definitions of scaling variables in the double angle method are:

$$Q_{DA}^2 = \frac{4E_l^2 \cos^2 \frac{\theta_l}{2}}{\sin^2 \frac{\theta_l}{2} + \sin \frac{\theta_l}{2} \cos \frac{\theta_l}{2} \tan \frac{\theta_h}{2}}, \quad (\text{A.26})$$

$$y_{DA} = 1 - \frac{\sin \frac{\theta_l}{2}}{\sin \frac{\theta_l}{2} + \cos \frac{\theta_l}{2} \tan \frac{\theta_h}{2}}, \quad (\text{A.27})$$

$$x_{DA} = \frac{Q_{DA}^2}{Sy_{DA}}. \quad (\text{A.28})$$

θy method, [7]:

A quite similar opportunity is to express the cross sections in terms of θ_e in the laboratory system and y_{JB} . The kinematical variables are:

$$Q_{\theta y}^2 = 4E_e^2(1 - y_{JB}) \frac{1 + \cos \theta_l}{1 - \cos \theta_l}, \quad (\text{A.29})$$

$$y_{\theta y} = y_{JB}, \quad (\text{A.30})$$

$$x_{\theta y} = \frac{Q_{\theta y}^2}{Sy_{\theta y}}. \quad (\text{A.31})$$

Initial state radiation					
	\hat{S}	\hat{Q}^2	\hat{y}	z_0	$J(x, y, z)$
leptonic variables	Sz	$Q_l^2 z$	$\frac{z + y_l - 1}{z}$	$\frac{1 - y_l}{1 - x_l y_l}$	$\frac{y_l}{z + y_l - 1}$
mixed variables	Sz	$Q_l^2 z$	$\frac{y_{JB}}{z}$	y_{JB}	1
hadronic variables	Sz	Q_h^2	$\frac{y_h}{z}$	y_h	$\frac{1}{z}$
JB variables	Sz	$\frac{Q_{JB}^2 (1 - y_{JB}) z}{z - y_{JB}}$	$\frac{y_{JB}}{z}$	$\frac{y_{JB}}{1 - x_{JB}(1 - y_{JB})}$	$\frac{1 - y_{JB}}{z - y_{JB}}$
double angle method	Sz	$Q_{DA}^2 z^2$	y_{DA}	0	z
θ_l, y_{JB}	Sz	$Q_{\theta_l}^2 \frac{z(z - y_{JB})}{1 - y_{JB}}$	$\frac{y_{JB}}{z}$	y_{JB}	$\frac{z - y_{JB}}{1 - y_{JB}}$
Σ method	Sz	Q_Σ^2	y_Σ	x_Σ	$\frac{1}{z}$
$e\Sigma$ method	Sz	$Q_l^2 z$	$y_{e\Sigma} z$	x_Σ	1

Table 1: The scaling properties of various sets of kinematical variables for leptonic initial state radiation. The different parameters are defined in appendix A.

Final state radiation					
	\hat{S}	\hat{Q}^2	\hat{y}	z_0	$\mathcal{J}(x, y, z)$
leptonic variables	S	$\frac{Q_L^2}{z}$	$\frac{z + y_l - 1}{z}$	$1 - y_l(1 - x_l)$	$\frac{y_l}{z(z + y_l - 1)}$
mixed variables	S	$\frac{Q^2}{z}$	y_{JB}	x_m	$\frac{1}{z}$
Σ method	S	$Q_\Sigma^2 \frac{1 - y_\Sigma(1 - z)}{z^2}$	$\frac{y_\Sigma z}{1 - y_\Sigma(1 - z)}$	$z_0^{\Sigma,f}$	$\frac{1}{z^2}$
$e\Sigma$ method	S	$\frac{Q^2}{z}$	$\frac{y_{e\Sigma} z^2}{[1 - y_{e\Sigma}(1 - z)]^2}$	$z_0^{\Sigma,f}$	$\frac{1 + y_{e\Sigma}(1 - z)}{[1 - y_{e\Sigma}(1 - z)]z}$

Table 2: The scaling properties of various sets of kinematical variables for leptonic final state radiation. The different parameters are defined in appendix A.

$O(\alpha^2 L^2)$

$$\frac{d^2 \sigma^{ini, 2loop}}{dxdy} = \left[\frac{\alpha}{2\pi} L_e \right]^2 \int_0^1 dz P_{ee}^{(2,1)}(z) \left\{ \theta(z - z_0) \mathcal{J}(x, y, z) \frac{d^2 \sigma^{(0)}}{dxdy} \Big|_{x=\hat{x}, y=\hat{y}, S=\hat{S}} - \frac{d^2 \sigma^{(0)}}{dxdy} \right\}$$

$$+ \left(\frac{\alpha}{2\pi} \right)^2 \int_{z_0}^1 dz \left\{ L_e^2 P_{ee}^{(2,2)}(z) + L_e \sum_{f=l,q} \ln \frac{Q^2}{m_f^2} P_{ee,f}^{(2,3)}(z) \right\} \mathcal{J}(x, y, z) \frac{d^2 \sigma^{(0)}}{dxdy} \Big|_{x=\hat{x}, y=\hat{y}, S=\hat{S}}$$

The second order splitting functions are:

$$P_{ee}^{(2,1)}(z) = \frac{1}{2} [P_{ee}^{(1)} \otimes P_{ee}^{(1)}](z)$$

$$= \frac{1+z^2}{1-z} \left[2 \ln(1-z) - \ln z + \frac{3}{2} \right] + \frac{1}{2}(1+z) \ln z - (1-z),$$

$$P_{ee}^{(2,2)}(z) = \frac{1}{2} [P_{e\gamma}^{(1)} \otimes P_{\gamma e}^{(1)}](z)$$

$$\equiv (1+z) \ln z + \frac{1}{2}(1-z) + \frac{2}{3} \frac{1}{z} (1-z^3),$$

$$P_{ee,f}^{(2,3)}(z) = N_c(f) Q_f^2 \frac{1}{3} P_{ee}^{(1)}(z) \theta \left(1 - z - \frac{2m_f}{E_e} \right).$$

The symbol \otimes in (2.100) and (2.101) denotes the Mellin convolution:

$$A(x) \otimes B(x) = \int_0^1 dx_1 \int_0^1 dx_2 \delta(x - x_1 x_2) A(x_1) B(x_2).$$

$O(\alpha^h L^h)$ $h > 2$ (exp)

$$\frac{d^2 \sigma^{(>2, soft)}}{dxdy} = \int_0^1 dz P_{ee}^{(>2)}(z, Q^2) \left\{ \theta(z - z_0) \mathcal{J}(x, y, z) \frac{d^2 \sigma^{(0)}}{dxdy} \Big|_{x=\hat{x}, y=\hat{y}, S=\hat{S}} - \frac{d^2 \sigma^{(0)}}{dxdy} \right\}, \quad (2.104)$$

with [40, 7]:

$$P_{ee}^{(>2)}(z, Q^2) = D_{NS}(z, Q^2) - \frac{\alpha}{2\pi} L_e \frac{2}{1-z} \left\{ 1 + \frac{\alpha}{2\pi} L_e \left[\frac{11}{6} + 2 \ln(1-z) \right] \right\}, \quad (2.105)$$

$$D_{NS}(z, Q^2) = \zeta(1-z)^{\zeta-1} \frac{\exp \left[\frac{1}{2} \zeta \left(\frac{3}{2} - 2\gamma_E \right) \right]}{\Gamma(1+\zeta)}, \quad (2.106)$$

$$\zeta = -3 \ln [1 - (\alpha/3\pi)L_e]. \quad (2.107)$$

If the charge of the final state electron is not recorded, also the conversion cross section

$$\frac{d^2 \sigma^{(2, e^- \rightarrow e^+)}}{dxdy} = \int_{z_0}^1 dz P(z, Q^2; e^- \rightarrow e^+) \mathcal{J}(x, y, z) \frac{d^2 \sigma^{(0)}}{dxdy} \Big|_{x=\hat{x}, y=\hat{y}, S=\hat{S}} \quad (2.108)$$

with the conversion rate

$$P(z, Q^2; e^- \rightarrow e^+) = \left(\frac{\alpha}{2\pi} \right)^2 L_e^2 P_{ee}^{(2,2)}(z) \quad (2.109)$$

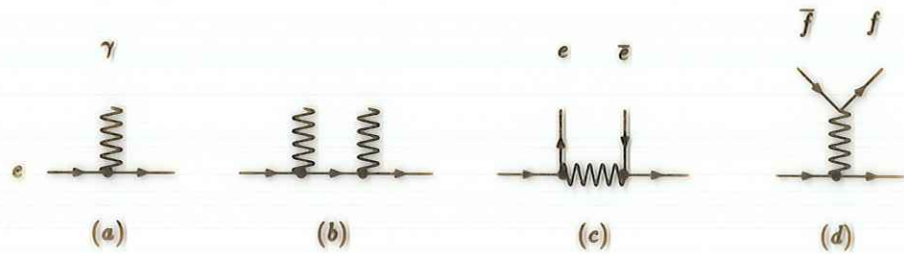


Figure 1: Diagrams contributing to the radiative corrections up to $\mathcal{O}(\alpha^2 L^2)$.

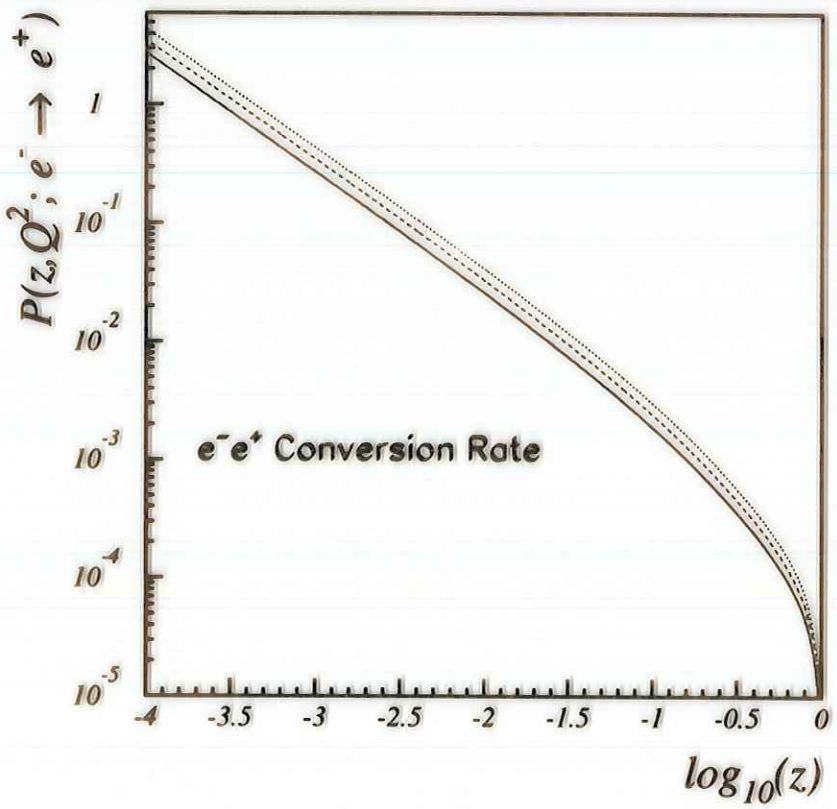


Figure 2: $e^- \rightarrow e^+$ transition rate for different values of Q^2 . Full line: $Q^2 = 10 \text{ GeV}^2$, dashed line: $Q^2 = 100 \text{ GeV}^2$, and dotted line: $Q^2 = 1000 \text{ GeV}^2$.

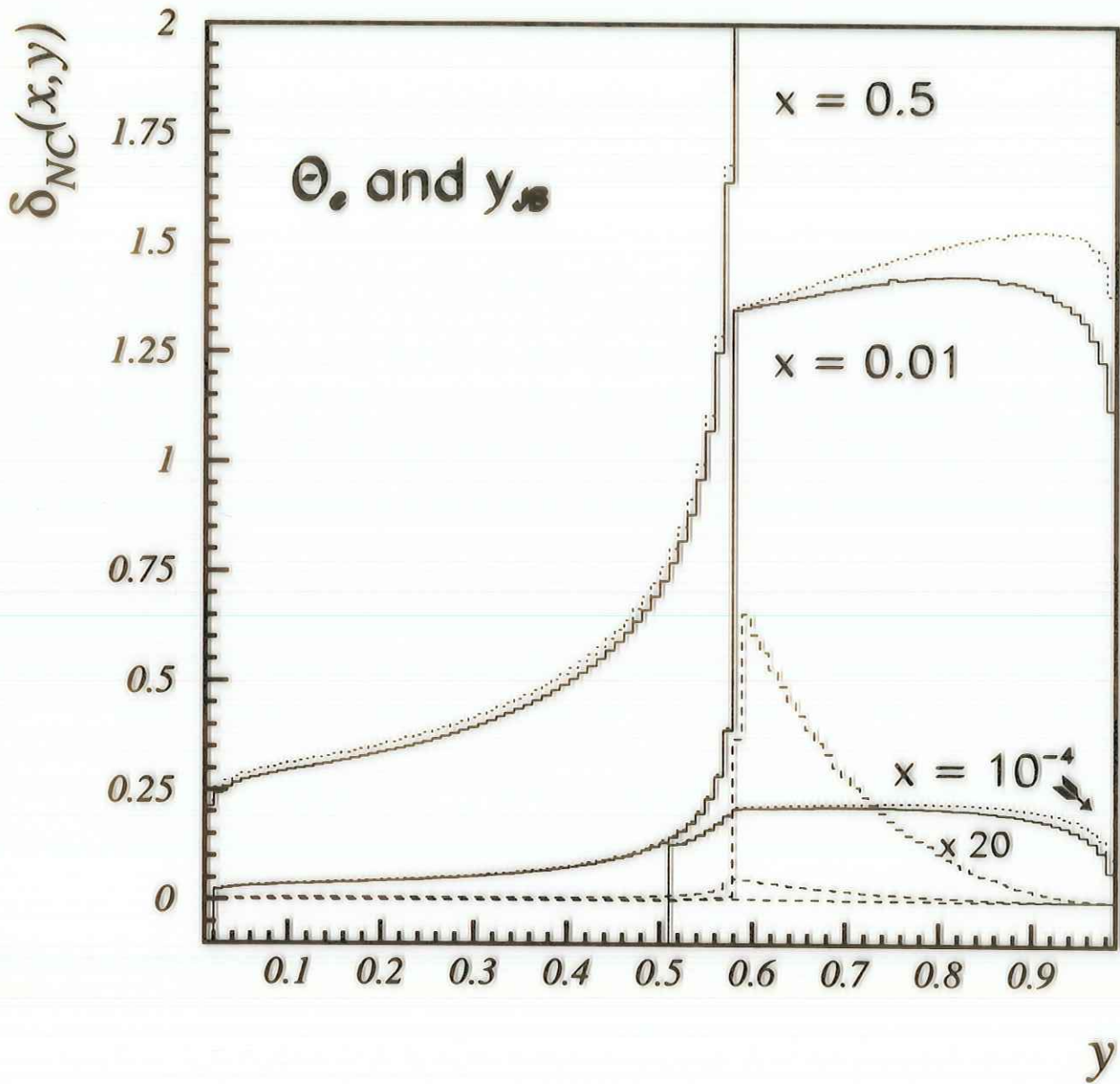


Figure 7: $\delta_{NC}(x, y)$ for the measurement based on θ_e and y_{JB} for $\mathcal{A} = 35 \text{ GeV}$. Full lines: $\delta_{NC}^{(1+2+>2,soft)}(x, y)$, dotted lines: $\delta_{NC}^{(1)}(x, y)$. Dashed lines: $\delta_{NC}^{e^- \rightarrow e^+}(x, y)$ scaled by $\times 20$; upper line: $x = 0.5$, middle line: $x = 10^{-2}$, lower line: $x = 10^{-4}$. The other parameters are the same as in figure 3.

Compton term

$$\frac{d^2\sigma^{C1}}{dx_l dy_l} = \frac{\alpha^3}{x_l S} [1 + (1 - y_l)^2] \ln \frac{Q_l^2}{M^2} \int_{z_l}^1 \frac{dz}{z^2} \frac{z^2 + (z_l - z)^2}{z_l(1 - y_l)} \sum_f [q_f(z, Q_l^2) + \bar{q}_f(z, Q_l^2)]. \quad (2.110)$$

$$\frac{d^2\sigma^{C2}}{dx_l dy_l} = \int_0^1 \frac{dz}{z} D_{\gamma/p}(z, Q_l^2) \left. \frac{d^2\hat{\sigma}(e\gamma \rightarrow e\gamma)}{dz dy_l} \right|_{z=zz, \hat{z}=z_l/z} \quad (2.111)$$

with

$$\frac{d^2\hat{\sigma}(e\gamma \rightarrow e\gamma)}{dz dy_l} = \frac{2\pi\alpha^2}{\hat{s}} \frac{1 + (1 - y_l)^2}{1 - y_l} \delta(1 - \hat{z}) \quad (2.112)$$

$$D_{\gamma/p}(z_l, Q_l^2) = \frac{\alpha}{2\pi} \int_{z_l}^1 dz \int_{Q_h^2, \min}^{Q_l^2} \frac{dQ_h^2}{Q_h^2} \frac{z}{z_l} \left[\frac{1 + (1 - z)^2}{z^2} F_2 \left(\frac{z_l}{z}, Q_h^2 \right) - F_L \left(\frac{z_l}{z}, Q_h^2 \right) \right]. \quad (2.113)$$

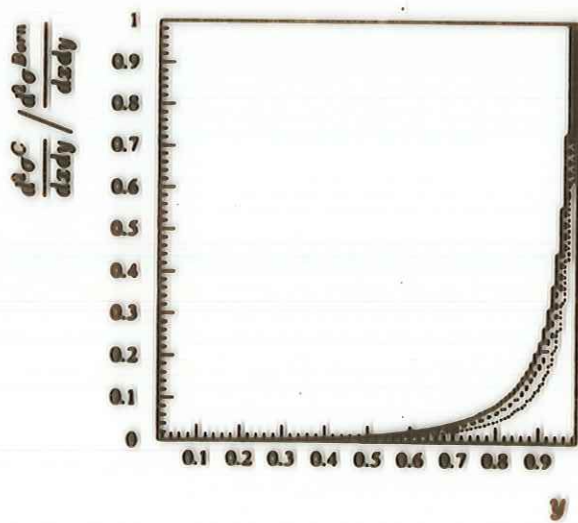


Figure 1: Differential Compton cross section Eq. (8) as a function of y_l for $x_l = 10^{-4}$ (dotted line), 10^{-3} (dashed line), and 10^{-2} (full line).

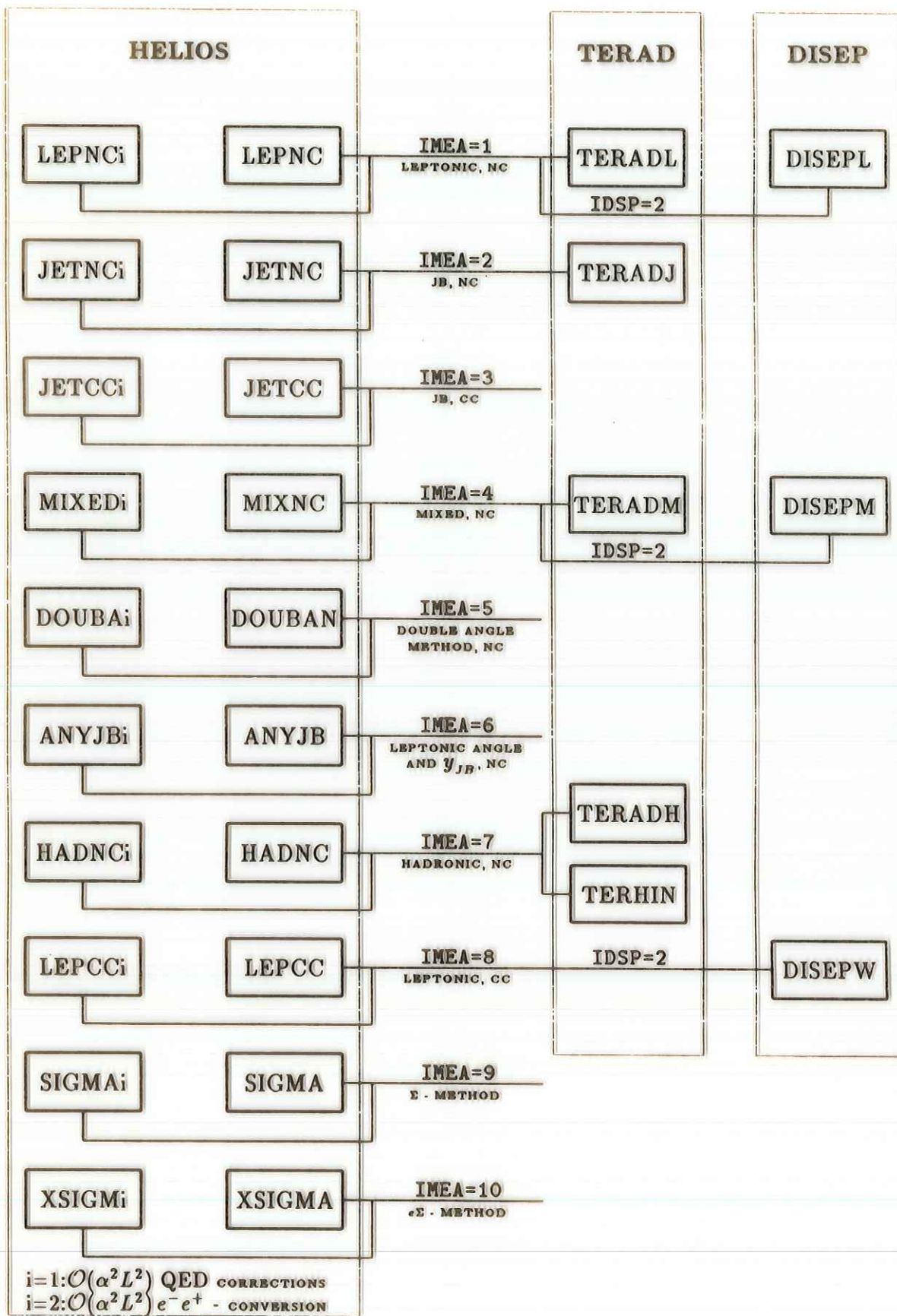


Figure 9: The branches of HECTOR. Different treatments of QED corrections are chosen by settings of flags IMEA and IDSP.

IMEA	ICOR	IDSP	IOPT	σ_B [nb]	$\delta^{(1)}$ [%]	$\delta^{(2)}$ [%]	δ^{all} [%]	Comments
1	1	0	1	0.2246E+06	13.01	-4092	12.60	$E_{\text{cut}} = 35 \text{ GeV}$ $E_{\text{cut}} = 35 \text{ GeV}$
2	1	0	1	0.2246E+06	3.928	.3942	4.322	
3	1	0	1	0.1066E+01	-0.837	.4420	.3583	
4	1	0	1	0.2246E+06	10.22	.6968	10.92	
5	1	0	1	0.2246E+06	5.512	.2490	5.761	
6	1	0	1	0.2246E+06	6.182	.2334	6.416	
7	1	0	1	0.2246E+06	4.469	.4151	4.884	
8	1	0	1	0.1066E+01	3.172	-.1664	3.006	
9	1	0	1	0.2246E+06	4.150	.5021	4.652	
10	1	0	1	0.2246E+06	9.328	2.492	11.82	
1	2	0	1	0.2246E+06	4.643			ICMP=1 ICMP=2
4	2	0	1	0.2246E+06	-2.687			
9	2	0	1	0.2246E+06	-2.873			
10	2	0	1	0.2246E+06	-3.040			
1	3	0	1	0.2246E+06	.02006			ICMP=1
				0.2246E+06	.02753			ICMP=2
1	1	0	2,3	0.2246E+06	17.82		17.41	
2	1	0	2,3	0.2246E+06	3.748		4.133	
4	1	0	2,3	0.2246E+06	7.195		7.783	
7	1	0	2,3	0.2246E+06	4.337		4.736	
1	1	1	2,3	0.2246E+06	17.82		17.41	
1	1	2	2,3	0.2246E+06	17.95		17.41	
4	1	1	2,3	0.2246E+06	7.189		7.783	
4	1	2	2,3	0.2246E+06	7.189		7.783	
8	1	1	2,3	0.1066E+01	8.100		7.933	IDIS=2
				0.1066E+01	8.070		7.903	IDIS=1

Table 6: Cross sections and radiative corrections for e^+p scattering as functions of flags IMEA, ICOR, IDSP, IOPT. Parameters: $x = 10^{-3}$, $y = 0.1$, $E_e = 26.7 \text{ GeV}$, $E_p = 820.0 \text{ GeV}$, and IVPL=1 (i.e. running α). The parton density parametrization CTEQ3L0 is chosen together with the low Q^2 damping factor corresponding to IVAR=0. Longitudinal structure functions are disregarded. For the $O(\alpha^2)$ corrections e^+e^- beam conversion terms were added. For IOPT=2 (3), the values of $\delta^{(i)}$ are given in columns 6(8).